Title: Nitrification and ammonium dynamics in Lake Taihu, China: seasonal competition for ammonium between nitrifiers and cyanobacteria.

Justyna J. Hampel[1*], Mark J. McCarthy[1,2], Wayne S. Gardner[2], Lu Zhang[3], Hai Xu[3], Guangwei Zhu[3], Silvia E. Newell[1]

[1] Department of Earth & Environmental Sciences, Wright State University, Dayton, OH
[2]The University of Texas at Austin, Marine Science Institute, Port Aransas, TX
[3]Taihu Laboratory for Lake Ecosystem Research, Nanjing Institute of Geography and Limnology, Chinese Academy of Sciences, Nanjing, China
[*] Corresponding author (hampel.4@wright.edu)

Abstract

Taihu Lake is hypereutrophic and experiences seasonal, cyanobacterial harmful algal blooms. These *Microcystis* blooms produce microcystin, a potent liver toxin, and are linked to anthropogenic nitrogen (N) and phosphorus (P) loads to lakes. *Microcystis spp.* cannot fix atmospheric N and must compete with ammonia-oxidizing and other organisms for ammonium (NH_4^+). We measured NH_4^+ regeneration and potential uptake rates and total nitrification using stable isotope techniques. Nitrification studies included abundance of the functional gene for NH_4^+ oxidation, *amoA*, for ammonia-oxidizing archaea (AOA) and bacteria (AOB). Potential NH_4^+ uptake rates ranged from 0.02–6.80 μmol L^{-1} h^{-1} in the light and 0.05–3.33 μmol L^{-1} h^{-1} in the dark, and NH_4^+ regeneration rates ranged from 0.03–2.37 μmol L^{-1} h^{-1}. Nitrification rates exceeded previously reported rates in most freshwater systems. Total nitrification often exceeded 200 nmol L^{-1} d^{-1} and was >1000 nmol L^{-1} d^{-1} at one station near a river discharge. AOA *amoA* gene copies were more abundant than AOB gene copies ($p < 0.005$) at all times; however, only abundance of AOB *amoA* (not AOA) was correlated with nitrification rates for all stations and all seasons ($p < 0.005$). Nitrification rates in Taihu varied seasonally; at most stations, rates were highest in March, lower in June, and lowest in July, corresponding with cyanobacterial bloom progression, suggesting that nitrifiers were poor competitors for NH_4^+ during the bloom. Regeneration results suggested that cyanobacteria relied extensively on regenerated NH_4^+ to sustain the bloom. Internal NH_4^+ regeneration exceeded external N loading to the lake by a factor of two but was ultimately fueled by external N loads. Our results thus support the growing literature calling for watershed N loading reductions in concert with existing management of P loads.

1. Introduction

Nitrogen (N) and phosphorus (P) are important nutrients in aquatic ecosystems, often co-limiting primary production (Elser et al., 2007). Biologically unavailable (except to diazotrophs) atmospheric N can be fixed to readily assimilable ammonium (NH_4^+) and biomass via N_2 fixation (Vitousek et al., 2013). However, fertilizer production from anthropogenic N fixation (the Haber-Bosch process) has changed N cycling and the global N budget over the last century. Non-point source N loads from agriculture are a main driver of eutrophication in aquatic systems, which is often manifested as hypoxia, loss of biodiversity, cyanobacterial harmful algal blooms (cyanoHABs; Paerl et al., 2016; Paerl and Paul, 2012), and other detrimental characteristics. CyanoHABs are particularly problematic because they often produce toxins, compete for nutrients with other microbes and primary producers, and indicate unhealthy aquatic systems.

The increase in extent and frequency of cyanoHABs correlates to increased application of NH_4^+ and urea fertilizers, both globally and in China (Glibert et al., 2014). Diatoms are competitive for oxidized forms of N (e.g., NO_3^-), but non-N_2 fixing cyanobacteria, such as *Microcystis*, thrive on chemically reduced N forms, such as NH_4^+ and urea (Blomqvist et al. 1994; Glibert et al., 2016; McCarthy et al., 2009). NH_4^+ transport across the cell membrane and assimilation into biomass is less energy intensive than for NO_3^- (Glibert et al., 2016). Due to high biological demand and fast turnover rates, NH_4^+ often does not accumulate in the water column, resulting in low *in situ* concentrations. Ammonium regeneration is especially important to phytoplankton productivity in eutrophic systems (Gardner et al. 1998, 2017; McCarthy et al., 2013). For example, water column regeneration was up to six times higher than sediment regeneration in Lake Taihu, China (McCarthy et al., 2007; Paerl et al., 2011).

Nitrification is the link between chemically reduced and oxidized N forms. Most nitrification pathways are a two-step process; NH_4^+ is oxidized to nitrite (NO_2^-) via ammonia oxidation, and NO_2^- is then oxidized to NO_3^- via NO_2^- oxidation. Ammonia oxidation is a rate limiting step (Ward, 2008) carried out by chemolithoautotrophic, ammonia oxidizing bacteria (AOB) and ammonia oxidizing archaea (AOA; Könneke et al., 2005). NO_2^- oxidation is carried out by NO_2^- oxidizing bacteria (NOB). Recently, a species of NOB was described that is capable of one step, complete nitrification ("comammox"); however, comammox bacteria have yet to be well documented in the environment (Daims et al., 2015). The ammonia and NO_2^- oxidation steps are often tightly coupled, where the product of the first step serves as a substrate for the second step (Ward, 2008). However, some studies in marine environments suggest that the process can be decoupled, with one step outpacing the other (Füssel et al., 2012; Heiss and Fulweiler, 2016).

In Taihu, the abundance of ammonia oxidizing organisms (AOO) was investigated in sediments, where AOA outnumbered AOB, often by an order of magnitude (Wu et al., 2013; Zeng et al., 2012; Zhao et al., 2013). Another sediment study revealed that, while AOO were present at all sites, the distribution of AOA and AOB depended on lake trophic status (Hou et al., 2013). Abundance of AOA decreased, while AOB increased, with increasing trophic status, following the substrate concentration hypothesis presented in kinetic experiments (Martens-Habbena et al., 2009). A suite of environmental variables (substrate concentration, oxygen concentration, light intensity, pH, etc.) influences nitrification rates and AOO community composition, including AOA and AOB relative abundances (Bristow et al., 2015; Merbt et al., 2012; Ward, 2008)

Nitrification can be closely coupled in time and space to N removal via denitrification, particularly in shallow systems with tightly coupled benthic-pelagic interactions (An and Joye, 2001; Jenkins and Kemp, 1984). Microbial removal of excess N in eutrophic systems is a crucial process to mitigate excessive N loads, and substrate availability for denitrification can depend on nitrification. However, nitrifiers must compete with phytoplankton and other primary producers for NH_4^+. In eutrophic systems, this competition could help determine microbial community structure and cyanoHAB severity. Although both AOO and cyanobacteria, such as *Microcystis*, have a strong affinity for NH_4^+ (Martens-Habbena 2009; Baldia et al., 2009), we are unaware of measurements made when AOO and cyanobacteria were in direct competition. At some point in the bloom progression, cyanobacteria must outcompete AOO for available NH_4^+.

The overall objective of this study was to investigate seasonal NH_4^+ dynamics and the degree of competition between AOO and cyanobacteria in hypereutrophic Taihu. We measured community NH_4^+ uptake and regeneration rates, and nitrification rates, under different bloom conditions to help determine how cyanoHABs influence NH_4^+ fluxes. We compare these rates to: (1) investigate the competition for NH_4^+ between phytoplankton/cyanobacteria and nitrifying bacteria and archaea; (2) quantify the oxidation of NH_4^+ to NO_3^-, which is in turn available for removal via denitrification or assimilation by other organisms; (3) determine the fraction of NH_4^+ that is supplied within the system via water column regeneration/remineralization; and (4) characterize the community composition of AOO. We hypothesized that: (1) lower nitrification rates occur during cyanoHABs due to increased competition for NH_4^+; (2) rates of nitrification are higher in Taihu than in most coastal and marine systems due to high *in situ* substrate concentrations; (3) rapid NH_4^+ turnover increases with phytoplankton biomass; and (4) AOB outnumber AOA due to higher saturation concentrations.

2. Methods

2.1 Site description and time frame

Lake Tai (Taihu; from the Chinese for "Great Lake") is China's third largest freshwater lake. Due to industrial development and urbanization in the watershed, Taihu has shifted from a diatom-dominated, mesotrophic lake to a hypereutrophic lake experiencing cyanoHABs (Paerl et al., 2014; Qin et al., 2007). Historically, these blooms have been associated with toxin producing, non-N_2 fixing *Microcystis spp.,* which can form surface scums on the lake for up to 10 months per year (Chen et al., 2003; Duan et al., 2009; Ma et al., 2016; Otten and Paerl 2011). The surface blooms have a well-documented negative impact on fisheries, tourism, and local economies, including a drinking water shutdown in 2007 (Qin et al., 2007; Steffen et al., 2017; Xu et al., 2010).

Taihu is a large (2,338 km^2), shallow (mean depth = 1.9 m) lake in southeast China, situated in the Yangtze river delta about 150 km west of Shanghai. The lake is an important source of freshwater and resources for the ~40 million people within the watershed. Taihu has a complicated hydrology, with 172 rivers and channels connected to the lake (Qin et al., 2007). This network of rivers carries nutrient loads from agricultural runoff, factories, and household wastewater. Taihu has a relatively long residence time of approximately 280–300 days (Paerl et al., 2014; Xu et al., 2010).

Water samples were collected from four locations: Stations 1 and 3 in Meiliang Bay, Station 7 in the north-central part of the lake, and Station 10 on the western side of the lake basin (Fig. 1). In previous studies (e.g., McCarthy et al., 2007), sampling Stations 1, 3, and 7 followed a discharge gradient from the Liangxihe River in the northeast part of Meiliang Bay to the central lake, and Station 0 ("river") was located at the Liangxihe River discharge. However, in 2007, the

128 Yangtze River was diverted into Taihu in an effort to decrease the lake residence time and flush
129 *Microcystis spp.* and nutrients out of the lake (Qin et al., 2010). Diverted water from the Yangtze
130 River now flows into Gonghu Bay, the easternmost of the three northern bays. This diversion
131 resulted in intermittent flow reversals through Meiliang Bay, where the Liangxihe River now
132 mainly serves as an outflow. Since the discharge gradient from Station 1 to 7 was no longer
133 consistent in Meiliang Bay, Station 0 was replaced with a new river input (Station 10) on the
134 western side of the lake near the Dapugang River mouth. Environmental variables (temperature,
135 dissolved oxygen, pH, total dissolved solids (TDS), and chlorophyll a) were measured in situ at
136 each site using a YSI 6600 multi-sensor sonde.
137 Water samples were collected in August 2013, June 2014, March 2015, and July 2016.
138 Each of these sampling events corresponded with a pronounced *Microcystis* bloom at all sites
139 (Ma et al., 2016; Deng et al., 2014; Li et al., 2017; Su et al., 2017; Qian et al., 2017), except
140 Stations 7 and 10 in March 2015 (visual observation). Our sampling dates were representative of
141 seasonal conditions in the region, specific to this subtropical climate zone, and did not
142 correspond with any extreme weather patterns (e.g., typhoons, droughts). Temperature and
143 precipitation patterns were average for this climate region. Water was collected into 4 l carboys
144 at the surface (top 20 cm) and near-bottom (approximately 2 m depth) to investigate any changes
145 in nutrient dynamics associated with depth. Samples for nutrient analyses (NO_3^-, NO_2^-, o-PO_4^{3-},
146 and urea) were filtered immediately in the field using 0.2 µm nylon syringe filters (GE
147 Millipore) into 15 ml snap-cap tubes (Falcon) and stored frozen at -20°C. Nutrient samples were
148 analyzed on a Lachat QuikChem 8000 nutrient analyzer at the University of Texas Marine
149 Science Institute (UTMSI; Aug 2013, June 2014) or a Lachat 8500 nutrient analyzer at Wright
150 State University (WSU; March 2015, July 2016) according to manufacturer directions. Ambient

151 NH_4^+ concentrations were determined by ammonium retention time shift (AIRTS) high
152 performance liquid chromatography (HPLC) at UTMSI (Gardner et al., 1995). Briefly, the atom
153 % ^{15}N-NH_4^+ and total NH_4^+ concentration are determined by comparing the retention time shift
154 of the sample relative to the natural abundance NH_4^+ standard (Gardner et al., 1996)

155 **2.2 Water column NH_4^+ uptake and regeneration**

156 NH_4^+ uptake and regeneration rates were determined following the protocol of McCarthy
157 et al. (2013). Water collected in 4 l carboys was returned to the Taihu Laboratory for Lake
158 Ecosystem Research (TLLER) for isotope amendments and incubations. 500 ml from each
159 site/depth was amended with 98% $^{15}NH_4Cl$ (Isotec; concentration added 8–96 μM) and
160 distributed into six (triplicates for light and dark) 70 ml, clear tissue culture bottles (Corning;
161 McCarthy et al., 2007). The goal of the substrate additions in these uptake/regeneration
162 experiments was to add more-than-trace levels to ensure that all of the label was not taken up
163 during the incubations; our goal was to add the label concentration at an equivalent value to the
164 most recent monitoring data we could obtain for NH_4^+ concentrations, or at least 8 μM (even
165 when concentrations are low, recycling rates can be quite high). Dark bottles were wrapped with
166 thick aluminum foil. Initial samples (T_0) were withdrawn from each bottle with a rinsed syringe,
167 filtered (0.2 μm filters) immediately into 8 ml glass vials (Wheaton), and frozen until analysis at
168 UTMSI. Light and dark bottles were then submerged (approximate depth 0.2 m) in a mesh bag at
169 in situ light and temperature in the lake. After ~24 h, final samples (T_f) were filtered in the same
170 manner as the T_0 samples. Total NH_4^+ concentrations and atom % ^{15}N for all samples were
171 determined by AIRTS/HPLC (Bruesewitz et al., 2015; Gardner et al., 1995). Potential uptake and
172 actual regeneration rates were calculated using the Blackburn/Caperon isotope dilution model
173 (Blackburn, 1979; Caperon et al., 1979; McCarthy et al., 2013). The uptake rate is considered a

potential rate, which includes nitrification, assimilation, and other consumption processes, and regeneration is an actual rate that encompasses remineralization, decomposition of dead organic matter, heterotrophic excretion, respiration, biodegradation, and sloppy feeding by zooplankton (Saba et al., 2011).

2.3 Ammonia and nitrite oxidation rates

Nitrification rates were measured directly using the $^{15}NH_4^+$ tracer addition method. 500 ml of water from each station and depth was distributed into 750 ml polycarbonate bottles, enriched with a tracer amount (approximately 20% of the total pool) of 98% $^{15}NH_4Cl$ (Isotec), mixed thoroughly by inverting 10 times, and distributed into three 125 ml polycarbonate incubation bottles. Unenriched samples for each station and depth were distributed into 125 ml incubation bottles. Initial samples (T_0) were filtered using 0.22 μm syringe filters into 30 ml polycarbonate bottles and frozen until analysis. Final samples were collected as described after incubating for 24 h at in situ light and temperature. Samples were returned frozen to WSU for analysis.

Accumulation of $^{15}NO_2^-$ was measured using the sodium azide (NaN_3) reduction method (Heiss and Fulweiler, 2016; McIlvin and Altabet, 2005; Newell et al., 2011). Briefly, 7.5 ml from each sample was distributed into a 12 ml Exetainer vial (Labco, UK) and capped tightly. Each sample was then injected (with gastight syringe) with 0.25 ml of 1:1 (v:v) 2 M NaN_3 :20% CH_3COOH solution (previously purged with Ar for 30 min), followed by incubation for 1 h at 30 °C (McIlvin and Altabet, 2005). All NO_2^- accumulated in the sample from NH_3 oxidation was transformed chemically to N_2O. After 1 h, the reaction was stopped by injection of 0.15 ml of 10 M NaOH.

196 Accumulation of $^{15}NO_3^-$ was measured using the Cd reduction/NaN_3 reduction method
197 (Heiss and Fulweiler, 2016). Approximately 25 ml from each sample was transferred into 50 ml
198 centrifuge tubes. First, in situ NO_2^- was removed with 0.25 ml of 0.4 M sulfamic acid (H_3NSO_3).
199 After 10 min, the reaction was neutralized with 0.125 ml of 2 M NaOH (Granger and Sigman,
200 2009). NO_3^- was reduced to NO_2^- by addition of 100 mg of MgO, 6.6 g of NaCl, and 0.75–1 g of
201 acidified Cd powder to each sample, followed by 17 h incubation on a shaker table (McIlvin and
202 Altabet, 2005). Samples were centrifuged at 1000 x g for 15 min, and 7.5 ml of supernatant was
203 carefully transferred into 12 ml Exetainers. Cadmium-reduced NO_2^- was further reduced to N_2O
204 with the previously described NaN_3 method.
205 Samples were sent inverted to the University of California Davis Stable Isotope Facility
206 for isotopic analysis of $^{45/44}N_2O$ using a ThermoFinnigan GasBench + PreCon trace gas
207 concentration system interfaced to a ThermoScientific Delta V Plus isotope-ratio mass
208 spectrometer (Bremen, Germany). Nitrification rates were corrected for NaN_3 reduction
209 efficiency, and $^{15}NO_2^-$ production was calculated as:
210 $$NH_3\ Ox\ (\text{in nM day}^{-1}) = (([^{15}N/^{14}N * [NO_2^-])_{24h} - ([^{15}N/^{14}N * [NO_2^-])_{0h})/ \alpha * t$$
211 Where $\alpha = [^{15}NH_4^+] / ([^{15}NH_4^+] + [^{14}NH_4^+])$
212 And $^{15}NO_3^-$ production:
213 $$NO_2^-\ Ox\ (\text{in nM day}^{-1}) = (([^{15}N/^{14}N * [NO_3^-])_{24h} - ([^{15}N/^{14}N * [NO_3^-])_{0h})/ \alpha * t$$
214 Where $\alpha = [^{15}NO_2^-] / ([^{15}NO_2^-] + [^{14}NO_2^-])$
215 Total nitrification rates were calculated from the sum of $^{15}NO_2^-$ and $^{15}NO_3^-$ accumulation.
216 **2.4 Quantitative Polymerase Chain Reaction (qPCR)**
217 During the 2014–2016 sampling events, environmental DNA for AOO abundance was
218 collected using 0.2 μm Sterivex filters (EMD Millipore, MA, USA) and preserved with Ambion

RNAlater (Invitrogen, Carlsbad, CA, USA). Approximately 60–120 ml of site water was pushed through the filter for each station and depth and then stored filled with 5 mL RNAlater. Preserved filters were frozen at -80 ˚C and transported to WSU. DNA was extracted using the Gentra PureGene kit (Qiagen Inc., USA) extraction protocol with slight modifications (Newell et al., 2011). Sterivex filters were first washed with Phosphate Buffer Saline 1X Solution (Fisher BioReagents, USA) to remove any residual RNAlater. Lysis buffer (0.9 ml) and Proteinase K (4 µl) were added to the filters, followed by 1 h incubation at 55 °C and 1 h incubation at 65 °C. The solution was removed to a 1.5 ml tube, and the incubation was repeated with fresh lysis buffer and Proteinase K.

Concentration and purity of the DNA were measured spectrophotometrically (Nanodrop 2000, ThermoScientific). AOA were targeted with Arch-amoAF and Arch-amoAR primers targeting the 635 base pair (bp) region of the *amoA* gene, subunit A of the ammonia monooxygenase enzyme (AMO; Francis et al. 2005). Bacterial *amoA* was quantified using amoAF and amoA2R primers (Rotthauwe et al., 1997) to target the 491 bp region of *amoA*. qPCR standards were prepared by cloning the fragment of interest for AOA and AOB with the TOPO TA Cloning Kit (Invitrogen, USA), inserting it into a competent cell plasmid (One Shot E. coli cells, Invitrogen, USA), and isolating the plasmid containing the *amoA* gene using the UltraClean Standard Mini Plasmid Prep Kit (Mo Bio Laboratories Inc., Carlsbad, CA, USA).

AOA and AOB qPCR assays were conducted within a single 96 well plate for each year (2014, 2015, and 2016). Each run included three negative controls (no template), five standards from serial dilution in triplicates, and the environmental DNA samples in triplicate. Each sample and standard received 12.5 µl of SYBR green Fast Mastermix (Qiagen Inc., USA), 0.5 µl of each 100 µM primer, and 2–15 ng of template DNA.

All PCR work was performed in a PCR fume hood after cleaning the surface with DNAaway (ThermoScientific, USA) and engaging the UV light (20 min) to prevent contamination. qPCR protocol followed the method of Bollmann et al. (2014) for AOA (95 °C initial denaturation for 5 min, 95 °C denaturation for 30 sec, 53 °C annealing for 45 sec, and 72 °C extension for 1 min; 45 cycles) and AOB (95 °C initial denaturation for 5 min, 95 °C denaturation for 30 sec, 56 °C annealing for 45 sec, 72 °C extension for 1 min; 45 cycles), followed by the melting curve. Automatic settings for the thermocycler (Realplex, Eppendorf) were used to determine threshold cycle (Ct values), efficiency (85–95%), and a standard curve with R^2 values above 0.9. Gene copy number was calculated as (ng * number mol $^{-1}$)/ (bp * ng g^{-1} * g mol^{-1} of bp) and is reported in gene copies/ml of sample water. The detection limit was 980 copies/ml for AOB and 4807 copies/ml for AOA. These calculated detection limits do not represent the greatest sensitivity possible with our method, as the standard concentrations were selected to bracket the expected environmental concentrations. Indeed, our reported values are above the detection limit for both AOA (by two orders of magnitude) and AOB.

2.5 Statistical analysis

All statistical analyses were performed using RStudio software (R Version 3.3.1). Prior to statistical analysis, data were checked for normality using the Shapiro–Wilk normality test. The only variables that were normally distributed were DO, pH, and TDS. To explore potential environmental drivers of the rates, a multivariate correlation analysis was performed using the Kendall correlation method for nonparametric data. A p-value of <0.05 was considered statistically significant. Additionally, stepwise multiple regression models were run using the MASS package (R Version 7.3). The best fitting model was selected based on the minimum

Akaike's Information Criteria (AIC; Akaike 1974). To normalize data for parametric analysis, all non-normally distributed variables were log(x+1) transformed prior running the model.

3. Results

3.1 Lake ambient conditions

Physicochemical parameters in Taihu varied seasonally and spatially (Table 1). The most pronounced seasonal variations were observed in temperature and DO, with highest water temperature recorded in August. DO varied significantly, with highest values in March and lowest in August ($p < 0.01$). pH varied significantly with season, with lowest values in March and highest in August ($p < 0.01$). TDS values were highest in July 2016 and lowest in August 2013 ($p < 0.001$). Chlorophyll a concentrations were lowest in March 2015 (mean = 11.1 μg L^{-1}), but bloom conditions (> 20 μg L^{-1}; Xu et al., 2015) were observed at some locations (e.g., 20.3 μg L^{-1} at Station 3, and visual confirmation at Stations 1, 3, and several other areas of the lake). Bloom conditions were also present and observed at all sites in June 2014 (mean = 36.6 μg L^{-1}), July 2016 (mean = 58.1 μg L^{-1}), and August 2013 (43.7 μg L^{-1}).

Ammonium concentrations remained high throughout all sampling events, with highest values in March 2015 and lowest values in August 2013, but differences were not statistically significant ($p = 0.125$). Nitrite concentrations were not different between seasons, although they were significantly higher at Station 10 than other stations ($p < 0.001$). Nitrate concentrations followed the pattern of NH_4^+ concentrations and were highest in March 2015 and lowest in August 2013 ($p < 0.001$). Orthophosphate concentrations followed a seasonal pattern with lowest concentrations in March and highest in August ($p < 0.005$), and o-PO_4^{3-} concentrations at Station 10 were significantly higher than at any other station ($p < 0.001$).

3.2 Potential NH_4^+ uptake

In August 2013, light uptake rates (all NH_4^+ uptake are potential rates) were uniform across sites (mean = 0.40 ± 0.04 μmol L^{-1} h^{-1}) and did not vary between surface and bottom waters (Fig. 2a). In June 2014, light uptake rates in surface waters at Stations 1, 7, and 10 (mean = 0.80 ± 0.06 μmol L^{-1} h^{-1}) were significantly higher than deep rates (mean = 0.31 ± 0.08 μmol L^{-1} h^{-1}; $p < 0.001$). However, light uptake rates at Station 3 did not differ from zero at either depth (Fig. 2a). Mean surface and deep uptake rates in the dark in August 2013 (0.25 ± 0.01 μmol L^{-1} h^{-1}) and June 2014 (0.13 ± 0.05 μmol L^{-1} h^{-1}) were significantly lower than light uptake rates (Fig. 2b; $p < 0.05$). In March 2015, light uptake rates at Stations 1–7 (mean = 0.12 ± 0.04 μmol L^{-1} h^{-1}) were lower than those during August 2013 and June 2014 (mean = 0.43 ± 0.41 μmol L^{-1} h^{-1}) except for Station 10, where the rates were significantly higher (mean = 1.36 ± 0.20 μmol L^{-1} h^{-1}; $p < 0.001$). In contrast to summer, dark uptake rates in March 2015 were not significantly different than light rates (Fig. 2b). In July 2016, light uptake rates were highest at Stations 1, 7, and 10 (1.31 – 6.82 μmol L^{-1} h^{-1}). Stations 3 and 7 rates were highest in bottom waters (0.80 ± 0.16 μmol L^{-1} h^{-1} and 2.55 ± 0.14 μmol L^{-1} h^{-1}, respectively). In July 2016, light and dark uptake rates did not differ significantly ($p = 0.15$); highest dark uptake rates were observed at Station 1 in surface water (3.33 ± 0.67 μmol L^{-1} h^{-1}). Light uptake rates, across all stations and seasons, correlated positively with TDS and NH_4^+:NO_3^- and negatively with pH, while dark uptake rates correlated positively with TDS, NH_4^+, and NH_4^+:NO_3^-, and negatively with pH (Table 2).

3.3 Regeneration of NH_4^+

Regeneration rates in the light and dark (all NH_4^+ regeneration rates are actual rates, not potential) were not significantly different from each other across all years and seasons; therefore, light and dark rates were averaged together (Fig. 2c). Regeneration rates did not differ

311 significantly between the summer bloom sampling events in August 2013 and June 2014 (mean
312 = 0.22 ± 0.03 μmol L^{-1} h^{-1}), but July 2016 regeneration rates (mean = 0.75 ± 0.16 μmol L^{-1} h^{-1})
313 were significantly higher than in August and June ($p = 0.004$), with exceptionally high
314 regeneration rates occurring in surface waters in July at Station 1 (mean = 2.37 ± 0.16 μmol L^{-1}
315 h^{-1}). In March 2015, mean surface and deep regeneration rates decreased from the river mouth
316 (Station 10; 0.88 ± 0.15 μmol L^{-1} h^{-1}) towards the center of the lake, with significantly higher
317 regeneration rates at 10 than Stations 1–7 (mean = 0.10 ± 0.03 μmol L^{-1} h^{-1}; $p < 0.01$).
318 Regeneration rates were positively correlated with TDS, NH_4^+, and o-PO_4^{3-} concentrations, and
319 NH_4^+:NO_3^- (Table 2).

320 **3.4 Nitrification (2014-2016)**

321 Note that nitrification rates are presented in nmol L^{-1} d^{-1} for consistency with literature
322 reported values (Fig 3). At stations 1, 3, and 7 $^{15}NH_4^+$ additions, 91.8 % of the label was detected
323 as $^{15}NO_3^-$ and only 8.2 % as $^{15}NO_2^-$ (Fig 3a). Total nitrification rates at Station 3 did not vary
324 across seasons. At Station 7 in the central lake, highest total nitrification rates were observed in
325 March 2015 (mean = 663 ± 69.4 nmol L^{-1} d^{-1}) in both surface and deep waters compared to the
326 lowest rates in July 2016 (mean = 1.58 ± 0.78 nmol L^{-1} d^{-1}). At Station 1, the highest rates were
327 measured in surface waters in July 2016 (mean = 773 ± 50.7 nmol L^{-1} d^{-1}), but the rates at depth
328 followed a seasonal pattern from high in the spring (mean = 646 ± 158 nmol L^{-1} d^{-1}) to an order
329 of magnitude lower in the summer (mean = 9.86 ± 3.28 nmol L^{-1} d^{-1}).

330 Total nitrification rates at Station 10 were significantly higher than other stations (Fig.
331 3b; $p < 0.001$). Rates were, at times, orders of magnitude higher, and total nitrification ranged
332 from 148 – 3750 nmol L^{-1} d^{-1} (mean = 1590 ± 1390 nmol L^{-1} d^{-1}), compared to Stations 1–7

ranging from 2.00 – 771 nmol L^{-1} d^{-1} (mean = 270 ± 277 nmol L^{-1} d^{-1}). At Station 10 in July 2016, 80% of the $^{15}NH_4^-$ addition was detected as $^{15}NO_2^-$.

3.5 Ammonia oxidizer abundance

Abundance of the bacterial *amoA* gene for all years (2014–2016) varied from undetectable to 2.85 x 10^5 ± 5.20 x 10^4 copies ml^{-1}. Archaeal *amoA* abundance ranged from undetectable to 1.03 x 10^7 ± 3.37 x 10^6 copies ml^{-1} (Fig. 4a). Neither AOB nor AOA *amoA* gene copy abundances were statistically different between the three seasons. The highest ratio of AOB:AOA gene abundance (1.81) was reported at Station 3 in Meiliang Bay (Fig. 4b), and the lowest ratio (0.01) was observed at Station 7. AOB gene abundance was positively correlated with NH_4^+, NO_2^-, and o-PO_4^{3-} concentrations, and NH_4^+:NO_3^-, while AOA gene abundance was not significantly correlated to any environmental variable (Table 2).

4. Discussion

4.1 Ammonium regeneration and potential uptake

Ammonium uptake rates (0.02 – 6.82 μmol L^{-1} h^{-1}) reported here were within the range of or slightly higher than rates reported in other studies (Table 3). Rates were higher than uptake rates reported previously in Meiliang Bay (0.11 – 1.54 μmol L^{-1} h^{-1}) and the central lake (0.03 – 0.32 μmol L^{-1} h^{-1}) but within the range of rates reported in the Liangxihe River (0.70 – 4.19 μmol L^{-1} h^{-1}; McCarthy et al., 2007). Light uptake rates in March, June, and August resembled rates in eutrophic Lake Okeechobee but were higher than rates in Missisquoi Bay, Lake Champlain, Lake Michigan, and eutrophic New Zealand lakes Rotorua and Rotoiti (Table 3 and references therein). Higher light uptake rates were reported only in hypereutrophic Lake Maracaibo, Venezuela (Table 3) and in Maumee Bay, Lake Erie during a summer cynaoHAB bloom (Gardner et al. 2017). Potential NH_4^+ uptake rates in these systems, evaluated using the same

356 methods, increase with chlorophyll a ($p < 0.05$), but the proportion of community uptake that can
357 be supported by regeneration remains relatively consistent (Table 3).
358 Light uptake rates in Taihu were marginally higher ($p = 0.08$) than dark uptake rates,
359 presumably due to reduced photosynthetic phytoplankton activity. Photoautotrophs may continue
360 to assimilate nutrients in the dark under nutrient limitation (Cochlan et al., 1991), but Taihu is
361 generally nutrient replete, so we assume that dark uptake rates can be attributed mostly to
362 heterotrophic or chemolithoautotrophic organisms. Uptake rates were significantly higher in July
363 2016 than at other times, which may have been due to higher precipitation and subsequent
364 runoff; during summer 2016, average rainfall in June and July was about 305 mm compared to
365 106 mm in June 2014, 105 mm in August 2013, and 54 mm in March 2015
366 (WorldWeatherOnline.com; accessed on <08/02/2017>) however, it is within the range of typical
367 summer rainfall (185–320 mm; WorldWeatherOnline.com). Dark uptake rates in Taihu exceeded
368 dark rates reported in Lake Okeechobee (0.02 – 0.04 μmol L^{-1} h^{-1}; James et al. 2011), Missisquoi
369 Bay, Lake Champlain (0.10 μmol L^{-1} h^{-1}; McCarthy et al., 2013), and Lake Michigan (7 nmol L^{-1}
370 h^{-1}; Gardner et al., 2004) suggesting high activity of both heterotrophs and chemolithoautotrophs
371 in Taihu. A previous metagenomics study of the bloom composition in Taihu revealed an
372 overlooked contribution of heterotrophic bacteria to N assimilation processes by *Microcystis*,
373 which could be important in driving toxic blooms (Steffen et al., 2012).
374 Internal NH_4^+ cycling via regeneration is important in Taihu and varies seasonally (McCarthy
375 et al., 2007; Paerl et al., 2011). In March 2015, about 38% of light uptake for all sites and depths
376 was supported by regeneration (Fig. 2d). This proportion increased in June 2014 and July 2016
377 to 58% and 42%, respectively, and was highest in August 2013 (109%). The importance of
378 regeneration corresponded to decreasing in situ NH_4^+ concentrations (Fig. 2D). These results

379 suggest that, in March and June, regeneration supplemented ambient NH_4^+ in the water column
380 to support algal production, whereas cyanobacteria relied more heavily on NH_4^+ from
381 regeneration to sustain blooms in July and August. Water column regeneration may supply more
382 NH_4^+ for blooms than sediment NH_4^+ regeneration in Taihu due to combined spatial,
383 temperature, and biogeochemical factors (McCarthy et al., 2007; Gardner et al., 2017). Rapid
384 decomposition of cyanoHAB biomass may provide NH_4^+ for nitrification, which provides
385 substrate for denitrification. High rates of sediment denitrification (McCarthy et al., 2007) also
386 may drive N limitation in late summer and fall (Paerl et al., 2011; Xu et al., 2010)
387 To calculate whole-lake, water column NH_4^+ regeneration and uptake rates, we divided the
388 lake (2,338 km^2; Qin et al., 2007) into four different sections based on geochemical and
389 ecological properties (Qin, 2008): (1) three northern bays (361.8 km^2; depth = 1.9 m) most
390 affected by the blooms; (2) the main lake (1,523.9 km^2; depth = 1.9 m); (3) the East Taihu
391 region, dominated by rooted and floating macrophytes (357.5 km^2; depth = 1.4 m); and (4)
392 shorelines <1 m deep (94.8 km^2). We considered regeneration and uptake rates from Stations 1
393 and 3 to represent the northern bays area, Station 7 as the main lake, Station 10 as shoreline, and
394 regeneration rates previously reported for East Taihu (McCarthy et al., 2007; Paerl et al., 2011).
395 When extrapolated to the volume of these four zones in Taihu, regeneration returned about 3.04
396 x 10^7 kg of NH_4^+ annually in the three northern bays, 6.71 x 10^7 kg of NH_4^+ in the main lake,
397 8.87 x 10^6 kg of NH_4^+ along the shorelines, and 2.88 x 10^6 kg of NH_4^+ in East Taihu Lake. These
398 values sum to 1.09 x 10^8 kg of NH_4^+recycled in the water column, approximately two times
399 higher than reported external N loadings, which range from 5.11 x 10^7 to 7.00 x 10^7 kg annually
400 (Chen et al., 2012; Yan et al., 2011). The same procedure for extrapolation of whole-lake uptake
401 rates yields 3.5 x 10^8 kg of NH_4^+, which is 4–6 times higher than external N loads. The

402 combination of external loads and regeneration cannot support the demand for NH_4^+, suggesting
403 that the remaining NH_4^+ demand must be satisfied by internal loads from sediments or some
404 other unknown source, or that reported TN loads are underestimated. These rough estimates of
405 lake-wide regeneration and uptake are based on rates measured at specific stations at discreet
406 times; improved spatial and temporal resolution of measurements are needed to improve these
407 estimates. Additionally, these calculated values are probably an overestimate given that most of
408 the rates measured and reported in this study are during spring and summer months, not fall and
409 winter, when we might expect lower rates. Taihu is a complex ecosystem with 172 rivers and
410 channels connected to the lake (Qin et al., 2007), making any estimations of total N loadings
411 challenging. As such, we believe that the reported total N loads to Taihu are likely an
412 underestimate. However, our results show that these external N loads lead to higher biomass and
413 fuel high regeneration rates. Combined with high ambient nutrient concentrations, these data
414 suggest that microbial denitrification cannot remove N fast enough to keep pace with external N
415 loading. Increasing nutrient loads can result in decreasing efficiency of denitrification (Gardner
416 and McCarthy, 2009; Mulholland et al., 2008), which will limit the ability of a system to self-
417 mitigate excess N loads.

418 **4.2 Nitrification**

419 Total nitrification rates reported in this study exceeded previously reported rates in most
420 oligotrophic and mesotrophic freshwater systems. Published nitrification rates in lakes include
421 the water columns of saline Lake Mono, CA (60–480 nmol L^{-1} d^{-1}; Carini and Joye, 2008) and
422 Lake Superior, USA (0–51 nmol L^{-1} d^{-1}; Small et al., 2013), both measured via $^{15}NH_4^+$ tracer
423 additions, and Lake Okeechobee, FL (67–97 nmol L^{-1} h^{-1}; James et al., 2011), measured via the
424 $^{15}NO_3^-$ pool dilution method (Carini et al., 2010). Rates on this scale were previously reported

425 only in eutrophic Lake Mendota (WI; 1700 – 26000 nmol L^{-1} h^{-1}; Hall, 1986) and the Paerl River
426 Estuary (China; 2100 – 65100 μmol L^{-1} d^{-1}; Dai et al., 2008). However, these rates were
427 measured from accumulation of NO_2^- and NO_3^-, not stable isotope additions. High total
428 nitrification rates in Taihu can be attributed to high ambient NH_4^+ concentrations, up to 40 μM at
429 Station 1 in 2016 and 135 μM at Station 10 in 2014. These high concentrations of NH_4^+ are due
430 to high external N loadings, including N in organic matter, into the lake, of which ~1.32 x 10^7 kg
431 were loaded as NH_4^+ in 2009 (Yan et al., 2011). The significant relationships between
432 nitrification and NH_4^+, NO_2^-, and NO_3^- concentrations ($p < 0.05$; Table 2) support these
433 observations.
434 Substrate concentrations drive NH_4^+ oxidation rates and, therefore, end-product pools,
435 since it is the rate limiting step of nitrification (i.e., completion of nitrification is dependent on
436 the first step). Accumulation of $^{15}NO_3^-$ exceeded accumulation of $^{15}NO_2^-$ by a factor of 9 at
437 Stations 1, 3, and 7 across all sampling events (Fig. 3a), indicating that NO_2^- oxidation is keeping
438 pace with or exceeding NH_4^+ oxidation. Higher accumulation of $^{15}NO_3^-$ was expected, since
439 NO_3^- is the final product of total nitrification.
440 At Station 10, accumulation of $^{15}NO_3^-$ exceeded $^{15}NO_2^-$ in March 2015 and June 2014. In
441 July 2016, however, accumulation of $^{15}NO_2^-$ was three times higher in surface water and
442 comparable at depth (Fig. 3b). Ambient NO_2^- concentration at Station 10 in July 2016 was 9.6
443 μM in surface water and 8.4 μM at depth (Table 1). This accumulation of NO_2^- suggests that
444 NO_2^- oxidizers were saturated, consistent with K_m values reported for NO_2^- oxidation in the
445 oligotrophic open ocean were 0.25 ± 0.16 μM (Sun et al., 2017). However, culture experiments
446 report K_m values ranging from 6–544 μM for *Nitrospira, Nitrobacter,* and *Nitrotoga spp.*
447 (Blackburne et al., 2007; Nowka et al., 2015; Ushiki et al., 2017).

448 At most stations, nitrification rates in Taihu were highest in March, lower in June, and lowest
449 in July. During the spring sampling, nitrification accounted for about 8% of light uptake and
450 15% of dark uptake at Stations 1 – 7. In June, nitrification accounted for 2.6% of light uptake
451 and 9.6% of dark uptake, and in July only 0.2% and 0.3% of light and dark uptake, respectively.
452 These results show a seasonal trend of decreasing contribution of nitrification to total uptake
453 rates and higher contribution of nitrifiers to dark uptake. As stated above, chemolithoautotrophs
454 (including nitrifiers) do not rely on light for energy and continue to assimilate NH_4^+ in dark
455 conditions, while photoautotrophic cyanobacteria can assimilated NH_4^+ in the dark only when
456 nutrient limited (Cochlan et al., 1991). However, the presence of high dissolved inorganic N
457 concentrations in ambient water samples suggests that the observed dark uptake was likely
458 performed primarily by non-photoautotrophs, including nitrifiers.
459 We observed no significant seasonal change in nitrification across all stations and no
460 consistent pattern between temperature and nitrification. While the lack of relationship of
461 nitrification with temperature agrees with nitrification studies in the ocean (Ward, 2008), other
462 studies have reported temperature as a potential driver of nitrification in coastal waters (Heiss
463 and Fulweiler, 2016). Although not statistically linked to changes in temperature, the
464 contribution of nitrification to total uptake rates decreased in summer months, likely as a result
465 of competition with the *Microcystis* bloom and associated heterotrophic bacteria. Non-N_2 fixing
466 cyanobacteria, including *Microcystis,* are exceptional competitors for NH_4^+ in high nutrient
467 environments (Blomqvist et al., 1994). With a high saturation threshold and reported K_m values
468 from 26.5 μM to 37 μM (Baldia et al., 2007; Nicklisch and Kohl 1983) in culture, and up to
469 112.9 μM in Taihu populations (Yang et al., 2017), *Microcystis* should be able to outcompete
470 nitrifiers at the high ambient NH_4^+ concentrations in Taihu as nitrifiers may become saturated as

much lower concentrations. Additionally, *Microcystis* can regulate its buoyancy and scavenge nutrients throughout the water column to effectively compete for light with other phytoplankton (Brookes and Ganf, 2001).

Nitrification at Station 10 differed dramatically from other stations. Total nitrification rates were, at times, orders of magnitude higher than at other stations. Also, Station 10 did not follow the trend of decreasing nitrification contribution with the bloom. Nitrification accounted for 19% of light uptake and 64.8% of dark uptake in June and only 1.7% and 2%, respectively, in March. We speculate that Station 10 differs from other stations because of the large nutrient and suspended particle loads from the Dapugang River, the second largest inflow into the lake (Yan et al., 2011). Suspended particles from sediments could trigger heterotrophic and anaerobic processes at Station 10, including reduction of NO_3^- to NO_2^- (Krausfeldt et al., 2017; Yao et al. 2016). In fact, denitrification and anammox gene transcripts were observed recently in the water column at Station 10 (Krausfeldt et al., 2017). These authors also speculated that the discharge of suspended sediments from the river might play a role in coupling anaerobic and aerobic processes in the turbid water column, resulting in rapid cycling of reduced and oxidized forms of N. Nitrification is the link between introduction of reduced N into the system and the removal of N through denitrification. Therefore, the efficiency of nitrification is crucial to the removal of N from this hypereutrophic lake.

4.3 Ammonia oxidizer abundance

AOB and AOA coexist in the environment, and environmental variables shape the community structure. AOA often dominate in environments with low substrate concentrations, such as the open ocean or oligotrophic lakes (Beman et al., 2008; Bollmann et al., 2014; Newell et al., 2011), while AOB are often more abundant in nutrient rich waters and soils (Hou et al.,

494 2013; Jia and Conrad, 2009; Kowalchuk and Stephen, 2001; Verhamme et al., 2011). This
495 substrate concentration adaptation is dictated by different physiological abilities to assimilate
496 NH_4^+. Culture studies show that AOA have a very high affinity (low half saturation constant;
497 K_m) for NH_4^+, and in general are saturated faster than AOB (Martens-Habbena et al., 2009). The
498 low half saturation constant (K_m = 0.132 μM; Martens-Habbena et al., 2009) of AOA gives them
499 a competitive advantage in low NH_4^+ conditions. In contrast, the high K_m of AOB (10–1000 μM)
500 allows them to assimilate more NH_4^+ before becoming fully saturated, an advantage for higher
501 NH_4^+ concentration conditions. Although oligotrophic AOA appear to proliferate in the
502 environment (Francis et al., 2005), some species adapt to higher substrate concentrations (Jung et
503 al., 2011; Tourna et al., 2011).
504 Results from the *amoA* gene copy abundance analysis show that AOA were more abundant
505 than AOB across all stations and seasons in Taihu. Although this result does not support our
506 original hypothesis, the results agree with previous studies in the water column and sediments in
507 Taihu (Zeng et al., 2012), which reported higher AOA abundance ($4.91 \times 10^5 – 8.65 \times 10^6$ copies
508 g^{-1} sediment) than AOB ($3.74 \times 10^4 – 3.86 \times 10^5$ copies g^{-1} sediment) in Meiliang Bay. Similarly,
509 another Taihu sediment study showed more AOA than AOB in sediments at all 20 investigated
510 stations (Wu et al., 2010).
511 The differences in abundance of AOO between stations, represented as AOB:AOA, show
512 spatial variability between the more nearshore and central lake stations (Fig. 4b). In this study,
513 AOA were more abundant in the central lake (Station 7), whereas AOB were more abundant
514 closer to shore. Due to a higher affinity for substrate (lower K_m), AOA are likely more
515 competitive when nutrient concentrations are lower, such as in the open lake (mean offshore
516 NH_4^+ concentration = 3.69 μM). In contrast, AOB, with higher K_m, thrive at higher NH_4^+

517 concentrations at nearshore locations (mean nearshore NH_4^+ concentration = 31.3 μM). These
518 results agree with previous research in Taihu, where AOA outnumbered AOB in sediments at
519 mesotrophic sites, and AOB were more abundant at hypereutrophic locations (Hou et al., 2013).
520 Another study in Taihu sediments also reported that both AOA abundance and AOA:AOB were
521 negatively correlated with ambient NH_4^+ concentration (Wu et al., 2010). However, the data
522 reported in this study show no significant relationship between AOA abundance and NH_4^+, NO_2^-,
523 and NO_3^- concentrations (Table 2).
524 Despite AOA outnumbering AOB, AOB abundance was correlated with total nitrification
525 rates for all stations and all seasons ($p < 0.005$), but AOA abundance was not. This result agrees
526 with a previous study in Taihu sediments, where AOA were negatively correlated ($r = 0.53$, $p <$
527 0.05) with potential nitrification rates (0 – 3.0 μg NO_3^-N g^{-1} dry sediment; Hou et al., 2013). We
528 speculate that AOA oxidized NH_4^+ at lower rates due to oversaturation and inhibition and may
529 not have contributed as much as AOB to nitrification rates in our study. This conclusion was also
530 reached in Plum Island Sound (MA, USA), where abundance of archaeal *amoA* was higher than
531 bacterial, but potential nitrification rates did not correlate with AOA (Bernhard et al., 2010). The
532 authors hypothesized various scenarios, including inhibition of AOA due to high substrate
533 concentrations, competition for NH_4^+ with AOB, or AOA using an alternative energy source
534 (Bernhard et al., 2010). Our results support the interpretation that AOA are at a disadvantage
535 when competing with AOB for NH_4^+ in a hypereutrophic system and most likely did not play a
536 major role in observed nitrification in Taihu. Recent studies show that AOA can oxidize cyanate
537 (Palatinszky et al., 2015) and urea (Tolar et al., 2016), although growth and oxidation rates may
538 be slow. Therefore, AOA may play an expanded role in Taihu, beyond just NH_4^+ oxidation.
539 **4.4 Multiple regression model**

The best-fitting multiple regression models for N dynamics in Taihu (Table 4) supported the Kendall non-parametric analysis (Table 2). Ammonium uptake and regeneration rates and nitrification were correlated with ambient NH_4^+, NO_2^-, and NO_3^- concentrations. Additionally, the best-fitting models revealed that variables changing with season had major influences on the models (Table 4). For example, uptake in the light and dark and regeneration rates were positively influenced by temperature and DO and negatively by pH. However, the model for nitrification rates did not reveal that the seasonal variables, such as temperature, played a major role in the model.

5. Conclusions

This study highlights the importance of water column NH_4^+ regeneration in providing a large proportion of the substrate necessary to sustain cyanoHABs. The results also show that nitrification does not account for a large proportion of NH_4^+ demand during cyanoHABs in Taihu. We showed that nitrification rates were detectable during the bloom but decreased as the bloom progressed, suggesting that nitrifiers are weaker competitors for substrate than *Microcystis*. Also, seasonal changes in light and dark NH_4^+ uptake and nitrification rates showed that AOO are outcompeted by *Microcystis*. Extremely high nitrification rates at the river mouth (Station 10) differed from rates at other stations, suggesting that other processes, such as coupled nitrification/denitrification, might be important in suspended sediments. Previous studies reported coupled denitrification with nitrification in sediments (McCarthy et al., 2007). Functional gene analysis suggested that gene abundance does not necessarily reflect performance of the function in eutrophic lakes. We speculate that AOA are present in the lake but do not contribute proportionately to nitrification, suggesting that AOA might play another role in the lake.

563 Ammonium inflow into the lake is a large source of reduced N, but external inputs are
564 not the sole source. Extrapolated whole-lake regeneration rates in the water column were twice
565 as high as external N loadings into the lake. To mitigate harmful algal blooms, N loadings into
566 the lake must be reduced so that N can be efficiently removed through denitrification, instead of
567 being recycled in the water column. Our results support the recent calls for dual nutrient (N + P)
568 management strategies (Paerl et al., 2011) and highlight the importance of (chemically) reduced
569 N removal through nitrification and denitrification.

570
571
572 Acknowledgments
573
574 We thank Guang Gao for laboratory space at NIGLAS and Kaijun Lu and other graduate
575 students at NIGLAS and TLLER for help in the field and in the lab. We also thank Richard
576 Doucett at UC Davis Stable Isotope Facility for ^{15}N sample analysis, and Justin Myers, Megan
577 Reed, and Ashlynn Boedecker, at WSU for help with nutrient analysis. We also thank Daniel
578 Hoffman at WSU for valuable help with nitrification experiments and Elise Heiss for her input
579 on statistical analysis. This work was jointly supported by the International Science &
580 Technology Cooperation Program of China (2015DFG91980) and the National Natural Science
581 Foundation of China (41573076, 41771519).

582

References:

Akaike, H.: A new look at the statistical model identification, IEEE transactions on automatic control, 19(6), 716–723, 1974.

An, S. and Joye, S. B.: Enhancement of coupled nitrification-denitrification by benthic photosynthesis in shallow estuarine sediments, Limnol. Oceanogr., 46(1), 62–74, doi:10.4319/lo.2001.46.1.0062, 2001.

Baldia, S. F., Evangelista, A. D., Aralar, E. V. and Santiago, A. E.: Nitrogen and phosphorus utilization in the cyanobacterium Microcystis aeruginosa isolated from Laguna de Bay, Philippines, J. Appl. Phycol., 19(6), 607–613, doi:10.1007/s10811-007-9209-0, 2007.

Beman, J. M., Popp, B. N. and Francis, C. A.: Molecular and biogeochemical evidence for ammonia oxidation by marine Crenarchaeota in the Gulf of California., ISME J., 2(4), 429–441, doi:10.1038/ismej.2008.33, 2008.

Bernhard, A. E., Landry, Z. C., Blevins, A., De La Torre, J. R., Giblin, A. E. and Stahl, D. A.: Abundance of ammonia-oxidizing archaea and bacteria along an estuarine salinity gradient in relation to potential nitrification rates, Appl. Environ. Microbiol., 76(4), 1285–1289, doi:10.1128/AEM.02018-09, 2010.

Blackburn, T. H.: Method for Measuring Rates of NH(4) Turnover in Anoxic Marine Sediments, Using a N-NH(4) Dilution Technique., Appl. Environ. Microbiol., 37(4), 760–765, 1979.

Blackburne, R., Vadivelu, V. M., Yuan, Z. and Keller, J.: Kinetic characterisation of an enriched Nitrospira culture with comparison to Nitrobacter, Water Res., 41(14), 3033–3042, doi:10.1016/j.watres.2007.01.043, 2007.

Blomqvist, P., Petterson, A. and Hyenstrand, P.: Ammonium-nitrogen: a key regulatory factor causing dominance of non-nitrogen-fixing cyanobacteria in aquatic systems, Arch. Hydrobiol., 132(2), 141–164, 1994.

Bollmann, A., Bullerjahn, G. and McKay, R. M.: Abundance and diversity of ammonia-oxidizing archaea and bacteria in sediments of trophic end members of the laurentian Great Lakes, Erie and Superior, PLoS One, 9(5), doi:10.1371/journal.pone.0097068, 2014.

Bristow, L.A., Sarode, N., Cartee, J., Caro-Quintero, A., Thamdrup, B. and Stewart, F.J.: Biogeochemical and metagenomic analysis of nitrite accumulation in the Gulf of Mexico hypoxic zone, Limnol. Oceanogr., 60(5), 1733–1750, 2015.

Brookes, J.D. and Ganf, G.G.: Variations in the buoyancy response of Microcystis aeruginosa to nitrogen, phosphorus and light, J. Plankton res., 23(12), 1399–1411, 2001.

Bruesewitz, D. A., Gardner, W. S., Mooney, R. F. and Buskey, E. J.: Seasonal water column

NH_4^+ cycling along a semi-arid sub-tropical river/estuary continuum: Responses to episodic events and drought conditions, Ecosystems, 18(5), 792–812, doi:10.1007/s10021-015-9863-z, 2015.

Caperon, J., Schell, D., Hirota, J. and Laws, E.: Ammonium excretion rates in Kaneohe Bay, Hawaii, measured by a 15N isotope dilution technique, Mar. Biol., 54(1), 33–40, doi:10.1007/BF00387049, 1979.

Carini, S. a. and Joye, S. B.: Nitrification in Mono Lake, California: Activity and community composition during contrasting hydrological regimes, Limnol. Oceanogr., 53(6), 2546–2557, doi:10.4319/lo.2008.53.6.2546, 2008.

Carini, S. A., McCarthy, M. J. and Gardner, W. S.: An isotope dilution method to measure nitrification rates in the northern Gulf of Mexico and other eutrophic waters, Cont. Shelf Res., 30(17), 1795–1801, doi:10.1016/j.csr.2010.08.001, 2010.

Chen Y., Qin B., Teubner K., Dokulil M.: Long-term dynamics of phytoplankton assemblages: Microcystis-domination in Lake Taihu, a large shallow lake in China, J. Plankton res., 1988(4), 2003.

Chen, X.F., Chuai, X.M., Zeng, J., Liu, T. and Yang, L.Y.: Nitrogenous fluxes and its self-purification capacity in Lake Taihu, Huan jing ke xue= Huanjing kexue, 33(7), 2309–2314, 2012.

Cochlan, W. P., Harrison, P. J. and Denman, K. L.: Diel periodicity of nitrogen uptake by marine phytoplankton in nitrate- rich environments, Limnol. Oceanogr., 36(8), 1689–1700, 1991.
Dai, M., Wang, L., Guo, X., Zhai, W., Li, Q., He, B. and Kao, S. J.: Nitrification and inorganic nitrogen distribution in a large perturbed river/estuarine system: the Pearl River Estuary, China, Biogeosciences, 5(5), 1227–1244, doi:10.5194/bg-5-1227-2008, 2008.

Dai, M., Wang, L., Guo, X., Zhai, W., Li, Q., He, B. and Kao, S.J.: Nitrification and inorganic nitrogen distribution in a large perturbed river/estuarine system: the Pearl River Estuary, China, Biogeosciences Discussions, 5(2), 1545–1585, 2008.

Daims, H., Lebedeva, E. V, Pjevac, P., Han, P., Herbold, C., Albertsen, M., Jehmlich, N., Palatinszky, M., Vierheilig, J., Bulaev, A., Kirkegaard, R. H., Bergen, M. von, Rattei, T., Bendinger, B., Nielsen, P. H. and Wagner, M.: Complete nitrification by Nitrospira bacteria, Nature, 528(7583), 504–509, doi:10.1038/nature16461, 2015.

Deng, J., Qin, B., Paerl, H. W., Zhang, Y., Ma, J. and Chen, Y.: Earlier and warmer springs increase cyanobacterial (Microcystis spp.) blooms in subtropical Lake Taihu, China, Freshw. Biol., 59(5), 1076–1085, doi:10.1111/fwb.12330, 2014.

Duan, H., Ma, R., Xu, X., Kong, F., Zhang, S., Kong, W., Hao, J. and Shang, L.: Two-decade reconstruction of algal blooms in China's Lake Taihu, Environ. Sci. Technol., 43(10), 3522–3528, 2009.

Elser, J. J., Bracken, M. E. S., Cleland, E. E., Gruner, D. S., Harpole, W. S., Hillebrand, H., Ngai, J. T., Seabloom, E. W., Shurin, J. B. and Smith, J. E.: Global analysis of nitrogen and phosphorus limitation of primary producers in freshwater, marine and terrestrial ecosystems, Ecol. Lett., 10(12), 1135–1142, doi:10.1111/j.1461-0248.2007.01113.x, 2007.

Francis, C. A., Roberts, K. J., Beman, J. M., Santoro, A. E. and Oakley, B. B.: Ubiquity and diversity of ammonia-oxidizing archaea in water columns and sediments of the ocean, Proc. Natl. Acad. Sci. U. S. A., 102(41), 14683–14688, doi:10.1073/pnas.0506625102, 2005.

Füssel, J., Lam, P., Lavik, G., Jensen, M. M., Holtappels, M., Günter, M. and Kuypers, M. M. M.: Nitrite oxidation in the Namibian oxygen minimum zone, ISME J., 6(6), 1200–1209, doi:10.1038/ismej.2011.178, 2012.

Gardner, W. S. and McCarthy, M. J.: Nitrogen dynamics at the sediment-water interface in shallow, sub-tropical Florida Bay: Why denitrification efficiency may decrease with increased eutrophication, Biogeochemistry, 95(2), 185–198, doi:10.1007/s10533-009-9329-5, 2009.

Gardner, W. S., Bootsma, H. A., Evans, C. and John, P. A. S.: Improved chromatographic analysis of 15N:14N ratios in ammonium or nitrate for isotope addition experiments, Mar. Chem., 48(3–4), 271–282, doi:10.1016/0304-4203(94)00060-Q, 1995.

Gardner, W.S., P.A. St. John, C. Evans, and J. Cavaletto.: HPLC retention-time-shift determination of nitrogen isotope ratios in enriched water. American Laboratory (Distinguished Authors' Issue) 28:17C-17H, 1996.

Gardner, W. S., Cavaletto, J. F., Bootsma, H. A., Lavrentyev, P. J. and Troncone, F.: Nitrogen cycling rates and light effects in tropical Lake Maracaibo, Venezuela, Limnololgy Oceanogr., 43(8), 1814–1825, 1998.

Gardner, W. S., Lavrentyev, P.J., Cavaletto, J.F., McCarthy, M.J., Eadie, B.J., Johengen, T.H. and Cotner, J.B.: Distribution and dynamics of nitrogen and microbial plankton in southern Lake Michigan during spring transition 1999–2000, J. Geophys. Res., 109(C3), C03007, doi:10.1029/2002JC001588, 2004.

Gardner, W.S., Newell, S.E., McCarthy, M.J., Hoffman, D.K., Lu, K., Lavrentyev, P.J., Hellweger, F.L., Wilhelm, S.W., Liu, Z., Bruesewitz, D.A. and Paerl, H.W.: Community Biological Ammonium Demand (CBAD): A Conceptual Model for Cyanobacteria Blooms in Eutrophic Lakes, Environ. Sci. Technol., 2017.

Glibert, P. M., Maranger, R., Sobota, D. J. and Bouwman, L.: The Haber Bosch–harmful algal bloom (HB–HAB) link, Environ. Res. Lett., 9(10), 105001, doi:10.1088/1748-9326/9/10/105001, 2014.

Glibert, P. M., Wilkerson, F. P., Dugdale, R. C., Raven, J. A., Dupont, C. L., Leavitt, P. R., Parker, A. E., Burkholder, J. M. and Kana, T. M.: Pluses and minuses of ammonium and nitrate uptake and assimilation by phytoplankton and implications for productivity and community composition, with emphasis on nitrogen-enriched conditions, Limnol. Oceanogr., 61(1), 165–

197, doi:10.1002/lno.10203, 2016.

Granger, J. and Sigman, D. M.: Removal of nitrite with sulfamic acid for nitrate N and O isotope analysis with the denitrifier method, Rapid Commun. Mass Spectrom., 23(23), 3753–3762, doi:10.1002/rcm.4307, 2009.

Hall, G.H.: Nitrification in lakes, in: Nitrification, 1st edition, edited by J. I. Prosser, IRL Press, Washington, DC, 127–156, 1986.

Heiss, E. M. and Fulweiler, R. W.: Coastal water column ammonium and nitrite oxidation are decoupled in summer, Estuar. Coast. Shelf Sci., 178, 110–119, doi:10.1016/j.ecss.2016.06.002, 2016.

Hou, J., Song, C., Cao, X. and Zhou, Y.: Shifts between ammonia-oxidizing bacteria and archaea in relation to nitrification potential across trophic gradients in two large Chinese lakes (Lake Taihu and Lake Chaohu), Water Res., 47(7), 2285–2296, doi:10.1016/j.watres.2013.01.042, 2013.

James, R. T., Gardner, W. S., McCarthy, M. J. and Carini, S. A.: Nitrogen dynamics in Lake Okeechobee: Forms, functions, and changes, Hydrobiologia, 669(1), 199–212, doi:10.1007/s10750-011-0683-7, 2011.

Jenkins, M. C. and Kemp, W. M.: The coupling of nitrification and denitrification in two estuarine sediments l v2, Limnol. Oceanogr., 29(3), 609–619, 1984.

Jia, Z. and Conrad, R.: Bacteria rather than Archaea dominate microbial ammonia oxidation in an agricultural soil, Environ. Microbiol., 11(7), 1658–1671, doi:10.1111/j.1462-2920.2009.01891.x, 2009.

Jung, M. Y., Park, S. J., Min, D., Kim, J. S., Rijpstra, W. I. C., Damst??, J. S. S., Kim, G. J., Madsen, E. L. and Rhee, S. K.: Enrichment and characterization of an autotrophic ammonia-oxidizing archaeon of mesophilic crenarchaeal group I.1a from an agricultural soil, Appl. Environ. Microbiol., 77(24), 8635–8647, doi:10.1128/AEM.05787-11, 2011.

Könneke, M., Bernhard, A. E., De La Torre, J. R., Walker, C. B., Waterbury, J. B. and Stahl, D. A.: Isolation of an autotrophic ammonia-oxidizing marine archaeon., Nature, 437(7058), 543–6, doi:10.1038/nature03911, 2005.

Kowalchuk, G. A. and Stephen, J. R.: Ammonia-oxidizing bacteria: a model for molecular microbial ecology, Annu. Rev. Microbiol., 55(1), 485–529, doi:10.1146/annurev.micro.55.1.485, 2001.

Krausfeldt, L. E., Tang, X., van de Kamp, J., Gao, G., Bodrossy, L., Boyer, G. L. and Wilhelm, S. W.: Spatial and temporal variability in the nitrogen cyclers of hypereutrophic Lake Taihu, FEMS Microbiol. Ecol., 93(4), 1–11, doi:10.1093/femsec/fix024, 2017.

768 Li, D. ming, Zheng, H. yan, Pan, J. lin, Zhang, T. qing, Tang, S. kai, Lu, J. ming, Zhong, L.
769 qiang, Liu, Y. shan and Liu, X. wei: Seasonal dynamics of photosynthetic activity, Microcystis
770 genotypes and microcystin production in Lake Taihu, China, J. Great Lakes Res., 43(4), 710–
771 716, doi:10.1016/j.jglr.2017.04.005, 2017.
772
773 Ma, J., Qin, B., Paerl, H. W., Brookes, J. D., Hall, N. S., Shi, K., Zhou, Y., Guo, J., Li, Z., Xu,
774 H., Wu, T. and Long, S.: The persistence of cyanobacterial (Microcystis spp.) blooms throughout
775 winter in Lake Taihu, China, Limnol. Oceanogr., 61(2), 711–722, doi:10.1002/lno.10246, 2016.
776
777 Martens-Habbena, W., Berube, P. M., Urakawa, H., De La Torre, J. R., Stahl, D. A. and Torre,
778 J.: Ammonia oxidation kinetics determine niche separation of nitrifying Archaea and Bacteria,
779 Nature, 461(7266), 976–979, doi:10.1038/nature08465, 2009.
780
781 McCarthy, M. J., Lavrentyev, P. J., Yang, L., Zhang, L., Chen, Y., Qin, B. and Gardner, W. S.:
782 Nitrogen dynamics and microbial food web structure during a summer cyanobacterial bloom in a
783 subtropical, shallow, well-mixed, eutrophic lake (Lake Taihu, China), Hydrobiologia, 581(1),
784 195–207, doi:10.1007/s10750-006-0496-2, 2007.
785
786 McCarthy, M. J., James, R. T., Chen, Y., East, T. L. and Gardner, W. S.: Nutrient ratios and
787 phytoplankton community structure in the large, shallow, eutrophic, subtropical Lakes
788 Okeechobee (Florida, USA) and Taihu (China), Limnology, 10(3), 215–227,
789 doi:10.1007/s10201-009-0277-5, 2009.
790
791 McCarthy, M. J., Gardner, W. S., Lehmann, M. F. and Bird, D. F.: Implications of water column
792 ammonium uptake and regeneration for the nitrogen budget in temperate, eutrophic Missisquoi
793 Bay, Lake Champlain (Canada/USA), Hydrobiologia, 718(1), 173–188, doi:10.1007/s10750-
794 013-1614-6, 2013.
795
796 McIlvin, M. R. and Altabet, M. A.: Chemical conversion of nitrate and nitrite to nitrous oxide for
797 nitrogen and oxygen isotopic analysis in freshwater and seawater, Anal. Chem., 77(17), 5589–
798 5595, doi:10.1021/ac050528s, 2005.
799
800 Merbt, S. N., Stahl, D. A., Casamayor, E. O., Marti, E., Nicol, G. W. and Prosser, J. I.:
801 Differential photoinhibition of bacterial and archaeal ammonia oxidation, FEMS Microbiol.
802 Lett., 327(1), 41–46, doi:10.1111/j.1574-6968.2011.02457.x, 2012.
803
804 Mulholland, P. J., Helton, A. M., Poole, G. C., Hall, R. O., Hamilton, S. K., Peterson, B. J.,
805 Tank, J. L., Ashkenas, L. R., Cooper, L. W., Dahm, C. N., Dodds, W. K., Findlay, S. E. G.,
806 Gregory, S. V, Grimm, N. B., Johnson, S. L., McDowell, W. H., Meyer, J. L., Valett, H. M.,
807 Webster, J. R., Arango, C. P., Beaulieu, J. J., Bernot, M. J., Burgin, A. J., Crenshaw, C. L.,
808 Johnson, L. T., Niederlehner, B. R., O'Brien, J. M., Potter, J. D., Sheibley, R. W., Sobota, D. J.
809 and Thomas, S. M.: Stream denitrification across biomes and its response to anthropogenic
810 nitrate loading., Nature, 452(7184), 202–205, doi:10.1038/nature06686, 2008.
811
812 Newell, S. E., Babbin, A. R., Jayakumar, D. A. and Ward, B. B.: Ammonia oxidation rates and
813 nitrification in the Arabian Sea, Global Biogeochem. Cycles, 25(4), 1–10,

814 doi:10.1029/2010GB003940, 2011.
815
816 Nicklisch, A. and Kohl, J.G.: Growth kinetics of Microcystis aeruginosa (Kütz) Kütz as a basis
817 for modelling its population dynamics, Internationale Revue der gesamten Hydrobiologie und
818 Hydrographie, 68(3), 317–326, 1983.
819
820 Nowka, B., Daims, H. and Spieck, E.: Comparison of oxidation kinetics of nitrite-oxidizing
821 bacteria: Nitrite availability as a key factor in niche differentiation, Appl. Environ. Microbiol.,
822 81(2), 745–753, doi:10.1128/AEM.02734-14, 2015.
823
824 Otten, T. G. and Paerl, H. W.: Phylogenetic Inference of Colony Isolates Comprising Seasonal
825 Microcystis Blooms in Lake Taihu, China, Microb. Ecol., 62(4), 907–918, doi:10.1007/s00248-
826 011-9884-x, 2011.
827
828 Paerl, H. W. and Paul, V. J.: Climate change: Links to global expansion of harmful
829 cyanobacteria, Water Res., 46(5), 1349–1363, doi:10.1016/j.watres.2011.08.002, 2012.
830
831 Paerl, H. W., Xu, H., McCarthy, M. J., Zhu, G., Qin, B., Li, Y. and Gardner, W. S.: Controlling
832 harmful cyanobacterial blooms in a hyper-eutrophic lake (Lake Taihu, China): The need for a
833 dual nutrient (N & P) management strategy, Water Res., 45(5), 1973–1983,
834 doi:10.1016/j.watres.2010.09.018, 2011.
835
836 Paerl, H. W., Xu, H., Hall, N. S., Zhu, G., Qin, B., Wu, Y., Rossignol, K. L., Dong, L.,
837 McCarthy, M. J. and Joyner, A. R.: Controlling cyanobacterial blooms in hypertrophic Lake
838 Taihu, China: Will nitrogen reductions cause replacement of non-N2 Fixing by N2 fixing taxa?,
839 PLoS One, 9(11), doi:10.1371/journal.pone.0113123, 2014.
840
841 Paerl, H. W., Gardner, W. S., Havens, K. E., Joyner, A. R., McCarthy, M. J., Newell, S. E., Qin,
842 B. and Scott, J. T.: Mitigating cyanobacterial harmful algal blooms in aquatic ecosystems
843 impacted by climate change and anthropogenic nutrients, Harmful Algae, 54, 213–222,
844 doi:10.1016/j.hal.2015.09.009, 2016.
845
846 Palatinszky, M., Herbold, C., Jehmlich, N., Pogoda, M., Han, P., von Bergen, M., Lagkouvardos,
847 I., Karst, S. M., Galushko, A., Koch, H., Berry, D., Daims, H. and Wagner, M.: Cyanate as an
848 energy source for nitrifiers., Nature, 524(7563), 105–8, doi:10.1038/nature14856, 2015.
849
850 Qian, H., Lu, T., Song, H., Lavoie, M., Xu, J., Fan, X. and Pan, X.: Spatial Variability of
851 Cyanobacteria and Heterotrophic Bacteria in Lake Taihu (China), Bull. Environ. Contam.
852 Toxicol., 99(3), 380–384, doi:10.1007/s00128-017-2149-8, 2017.
853
854 Qin, B. Q.: Lake Taihu, China: Dynamics and environmental change. Springer Netherlands,
855 2008.
856
857 Qin, B., Xu, P., Wu, Q. L., Luo, L. and Zhang, Y.: Environmental issues of Lake Taihu, China,
858 Hydrobiologia, 581(1), 3–14, doi:10.1007/s10750-006-0521-5, 2007.
859

Qin, B., Zhu, G., Gao, G., Zhang, Y., Li, W., Paerl, H. W. and Carmichael, W. W.: A drinking water crisis in Lake Taihu, China: Linkage to climatic variability and lake management, Environ. Manage., 45(1), 105–112, doi:10.1007/s00267-009-9393-6, 2010.

Rotthauwe, J.-H., Witzel, K.-P. and Liesack, W.: The Ammonia Monooxygenase Structural Gene amoA as a Functional Marker: Molecular Fine-Scale Analysis of Natural Ammonia-Oxidizing Populations, Appl. Environ. Microbiol., 63(12), 4704–4712, 1997.

Saba, G. K., Steinberg, D. K. and Bronk, D. A.: The relative importance of sloppy feeding, excretion, and fecal pellet leaching in the release of dissolved carbon and nitrogen by Acartia tonsa copepods, J. Exp. Mar. Bio. Ecol., 404(1–2), 47–56, doi:10.1016/j.jembe.2011.04.013, 2011.

Small, G. E., Bullerjahn, G., Sterner, R. W., Beall, B. F. N., Brovold, S., Finlay, J. C., McKay, R. M. and Mukherjee, M.: Rates and controls of nitrification in a large oligotrophic lake, Limnol. Oceanogr., 58(1), 276–286, doi:10.4319/lo.2013.58.1.0276, 2013.

Steffen, M. M., Li, Z., Effler, T. C., Hauser, L. J., Boyer, G. L. and Wilhelm, S. W.: Comparative Metagenomics of Toxic Freshwater Cyanobacteria Bloom Communities on Two Continents, PLoS One, 7(8), 1–9, doi:10.1371/journal.pone.0044002, 2012.

Steffen, M. M., Davis, T. W., McKay, R. M., Bullerjahn, G. S., Krausfeldt, L. E., Stough, J. M. A., Neitzey, M. L., Gilbert, N. E., Boyer, G. L., Johengen, T. H., Gossiaux, D. C., Burtner, A. M., Palladino, D., Rowe, M., Dick, G. J., Meyer, K., Levy, S., Boone, B., Stumpf, R., Wynne, T., Zimba, P. V, Gutierrez, D. B. and Wilhelm, S. W.: Ecophysiological examination of the Lake Erie Microcystis bloom in 2014 : linkages between biology and the water supply shutdown of Toledo, Ohio, Environ. Sci. Technol., doi:10.1021/acs.est.7b00856, 2017.

Su, X., Steinman, A. D., Xue, Q., Zhao, Y., Tang, X. and Xie, L.: Temporal patterns of phyto- and bacterioplankton and their relationships with environmental factors in Lake Taihu, China, Ecsn, 184, 299–308, doi:10.1016/j.chemosphere.2017.06.003, 2017.

Sun, X., Ji, Q., Jayakumar, A. and Ward, B.B.: Dependence of nitrite oxidation on nitrite and oxygen in low oxygen seawater. Geoph. Res Lett., 2017

Tolar, B. B., Wallsgrove, N. J., Popp, B. N. and Hollibaugh, J. T.: Oxidation of urea-derived nitrogen by thaumarchaeota-dominated marine nitrifying communities, Environ. Microbiol., 0(October), 1–13, doi:10.1111/1462-2920.13457, 2016.

Tourna, M., Stieglmeier, M., Spang, A., Könneke, M., Schintlmeister, A. and Urich, T.: Nitrososphaera viennensis, an ammonia oxidizing archaeon from soil, Proc. Natl. Acad. Sci. USA, 108(20), 8420–8425, doi:10.1073/pnas.1013488108/-/DCSupplemental.www.pnas.org/cgi/doi/10.1073/pnas.1013488108, 2011.

Ushiki, N., Jinno, M., Fujitani, H., Suenaga, T., Terada, A. and Tsuneda, S.: Nitrite oxidation kinetics of two Nitrospira strains: The quest for competition and ecological niche differentiation, J. Biosci. Bioeng., 123(5), 581–589, 2017.

Verhamme, D. T., Prosser, J. I. and Nicol, G. W.: Ammonia concentration determines differential growth of ammonia-oxidising archaea and bacteria in soil microcosms, ISME J., 5(6), 1067–1071, doi:10.1038/ismej.2010.191, 2011.

Vitousek, P. M., Menge, D. N., Reed, S. C. and Clevinger, C. C.: Biological nitrogen fixation: rates, patterns and ecological controls in terrestrial ecosystems, Philos. Trans. R. Soc. B Biol. Sci., 368(1621), 20130119, doi:10.1098/rstb.2013.0119, 2013.

Ward, B. B.: Nitrification in marine systems, in: Nitrogen in the Marine Environment, 2nd Edition, edited by: Capone, D., Bronk, D., Mulholland, M., and Carpenter, E., Elsevier, Amsterdam, 2008.

Wu, Y., Ke, X., Hernández, M., Wang, B., Dumont, M. G., Jia, Z. and Conrad, R.: Autotrophic growth of bacterial and archaeal ammonia oxidizers in freshwater sediment microcosms incubated at different temperatures, Appl. Environ. Microbiol., 79(9), 3076–3084, doi:10.1128/AEM.00061-13, 2013.

Xu, H., Paerl, H.W., Qin, B., Zhu, G. and Gaoa, G.: Nitrogen and phosphorus inputs control phytoplankton growth in eutrophic Lake Taihu, China. Limnol. Oceanogr., 55(1), 420–432, 2010.

Xu, H., Paerl, H. W., Qin, B., Zhu, G., Hall, N. S. and Wu, Y.: Determining critical nutrient thresholds needed to control harmful cyanobacterial blooms in eutrophic Lake Taihu, China, Environ. Sci. Technol., 49(2), 1051–1059, doi:10.1021/es503744q, 2015.

Yao, X., Zhang, L., Zhang, Y., Xu, H. and Jiang, X.: Denitrification occurring on suspended sediment in a large, shallow, subtropical lake (Poyang Lake, China). Environ. Pollut., 219, 501–511, 2016.

Yan, S., Yu, H., Zhang, L., Xu, J.: Water quantity and pollutant fluxes of inflow and outflow rivers of Lake Taihu, 2009, (Chinese). J. Lake Sci. 6, 855e862, 2011.

Yang, J., Gao, H., Glibert, P. M., Wang, Y. and Tong, M.: Rates of nitrogen uptake by cyanobacterially-dominated assemblages in Lake Taihu, China, during late summer, Harmful Algae, 65, 71–84, doi:10.1016/j.hal.2017.04.001, 2017.

Zeng, J., Zhao, D., Huang, R. and Wu, Q. L.: Abundance and community composition of ammonia-oxidizing archaea and bacteria in two different zones of Lake Taihu, Can. J. Microbiol., 58(8), 1018–1026, doi:10.1139/w2012-078, 2012.

Zhao, D., Zeng, J., Wan, W., Liang, H., Huang, R. and Wu, Q. L.: Vertical distribution of ammonia-oxidizing archaea and bacteria in sediments of a eutrophic lake, Curr. Microbiol., 67(3), 327–332, doi:10.1007/s00284-013-0369-7, 2013.

Figure list

Figure 1. Map of sampling stations in Taihu (modified from Paerl et al. 2011).

Figure 2. Ammonium dynamics in Taihu. (a) potential light uptake rates ± one standard error. (b) potential dark uptake rates ± one standard error. (c) Mean light and dark regeneration rates ± one standard error. (d) Seasonal averaged percent of light uptake supported by regeneration ± one standard error and averaged in situ NH_4^+ concentrations.

Figure 3. Total nitrification rates calculated from accumulation of $^{15}NO_2^-$ (grey) and $^{15}NO_3^-$ (black) ± one standard deviation. (a) Stations 1–7. (b) Station 10. The two axis show different units for total nitrification rates: nmol L^{-1} d^{-1} (left) and μmol L^{-1} h^{-1} (right).

Figure 4. Ammonia oxidizing organism population characteristics. (a) Ammonia oxidizer abundance (DNA) ± one standard deviation. (b) Ratio of abundance of AOB to AOA.

973 Table 1.
974 Environmental characteristics during sampling events for each station/depth: temperature,
975 dissolved oxygen (DO), pH, chlorophyll a (chl a; surface only), total dissolved solids (TDS), and
976 in situ nutrient concentrations. S in station name = surface water (0.2 m), and D = deep, near-
977 bottom water (~2 m).

Year/ Month	Station	Temp (°C)	DO (mg L^{-1})	pH	Chl a (µg L^{-1})	TDS	[NH_4^+] (µM)	[NO_2^-] (µM)	[NO_3^-] (µM)	[PO_4^{3-}] (µM)
2013	1S	30.9	3.53	8.11	53.9	377	1.37	0.28	2.09	2.51
	1D	30.8	4.24	8.05		377	1.79	0.23	2.17	2.96
	3S	32.5	9.07	9.02	57.6	390	0.51	0.23	1.84	1.64
	3D	31.9	7.40	8.97		390	0.56	0.25	0.60	1.62
	7S	30.4	3.40	8.05	22.2	357	0.26	0.21	2.20	0.41
	7D	30.4	3.40	8.18		357	0.32	0.14	0.90	2.73
	10S	32.1	8.60	9.33	40.8	375	0.61	1.90	7.74	4.83
	10D	32.0	8.00	9.43		375	0.29	1.04	3.76	5.69
2014	1S	23.9	8.50	8.11	13.7	436	6.16	3.33	87.5	1.75
	1D	22.7	5.10	8.07		437	8.34	3.36	87.1	0.69
	3S	27.2	8.60	8.73	11.1	419	1.09	1.72	58.3	0.24
	3D	25.4	7.30	8.71		411	1.20	2.61	57.4	0.35
	7S	22.8	9.70	7.85	42.4	383	1.55	0.83	66.3	0.39
	7D	22.5	8.60	7.69		384	1.59	0.74	61.6	2.13
	10S	26.3	5.60	8.89	79.5	424	35.4	14.9	70.0	2.43
	10D	26.4	5.50	8.60		424	35.7	15.1	68.9	2.52
2015	1S	11.6	10.1	8.34	7.5	393	2.49	0.55	53.9	0.20
	1D	11.7	3.40	6.67		393	2.49	0.58	54.7	0.04
	3S	9.4	12.8	7.74	20.4	414	BDL*	0.82	119.4	0.03
	3D	8.2	12.9	7.52		414	0.83	0.86	117.6	0.05
	7S	10.8	11.3	8.40	10.5	416	5.93	1.95	172.2	0.02
	7D	10.7	10.7	8.01		416	5.93	1.44	136.2	0.12
	10S	9.6	8.90	7.94	6.0	422	131	7.05	270.6	1.41
	10D	9.4	8.71	7.73		421	132	6.97	269.5	1.36
2016	1S	26.7	11.3	7.89	96.8	445	43.3	8.86	79.7	1.95
	1D	25.5	7.55	7.67		458	20.0	6.71	58.8	1.31
	3S	26.1	7.00	8.50	101.0	410	17.6	0.86	3.81	1.05
	3D	26.3	7.30	8.50		410	21.1	0.72	3.87	1.16
	7S	25.8	10.0	7.95	13.2	465	0.33	0.08	16.4	0.03
	7D	25.1	8.88	7.88		466	0.25	0.11	16.5	0.05
	10S	25.6	4.10	7.75	21.3	470	13.4	9.66	94.0	2.43
	10D	23.4	4.10	7.62		470	65.3	8.45	66.8	3.18

*Nutrient analysis detection limits: NH4+ = 0.04 µM; NOx = 0.04 µM; OP = 0.008 µM.

978

Table 2.
Details of non-parametric Kendall's correlation analysis. Statistically significant ($p < 0.05$) Kendall's Tau coefficients are bold.

		Temp	DO	pH	Chl a	TDS	NH_4^+	NO_2^-	NO_3^-	PO_4^{3-}	NH_4^+:NO_3^-
Uptake L	Kendall's T	-0.010	-0.061	**-0.326**	0.133	**0.321**	0.230	0.020	0.048	0.081	**0.301**
	p value	0.935	0.626	**0.009**	0.471	**0.010**	**0.064**	0.871	0.697	0.517	**0.016**
Uptake D	Kendall's T	-0.014	-0.041	**-0.293**	0.117	**0.337**	**0.295**	0.000	0.069	0.069	**0.369**
	p value	0.910	0.745	**0.019**	0.529	**0.007**	**0.018**	1.000	0.581	0.581	**0.003**
Regeneration	Kendall's T	0.095	-0.110	-0.103	0.300	**0.301**	**0.344**	0.149	0.012	**0.259**	**0.487**
	p value	0.446	0.381	0.408	0.105	**0.016**	**0.006**	0.230	0.923	**0.038**	**<0.001**
Nitrification	Kendall's T	-0.138	-0.128	-0.214	0.242	-0.058	**0.385**	**0.341**	**0.377**	**0.341**	0.272
	p value	0.346	0.385	0.143	0.273	0.691	**0.009**	**0.020**	**0.010**	**0.020**	0.063
AOA	Kendall's T	0.109	0.179	0.083	0.273	0.161	0.015	-0.014	-0.051	0.043	-0.004
	p value	0.457	0.224	0.568	0.217	0.275	0.921	0.921	0.728	0.766	0.980
AOB	Kendall's T	0.175	-0.157	-0.149	0.273	0.175	**0.458**	**0.341**	0.130	**0.500**	**0.425**
	p value	0.234	0.286	0.309	0.217	0.233	**0.002**	**0.020**	0.372	**0.001**	**0.004**

Table 3.
Comparison of ammonium dynamics (in μmol L^{-1} hr^{-1}) and chlorophyll a concentrations among different freshwater studies.

	Uptake (Light)	Uptake (Dark)	Regeneration	Chl a (μg L^{-1})	Reference
Lake Lugano	0.017 ± 0.001	0.008 ± 0.003	0.010 ± 0.002	< 2.00	McCarthy unpublished
Lake Michigan	0.019 ± 0.004	0.01 ± 0.002	0.008 ± 0.001	2.44	Gardner et al., 2004
Lake Rotorua	0.114 ± 0.008	0.021 ± 0.005	0.047 ± 0.007	23.3	Gardner et al., 2017
Lake Rotoiti	0.132 ± 0.033	0.08 ± 0.019	0.063 ± 0.018	7.66	Gardner et al., 2017
Missisquoi Bay	0.205 ± 0.022	0.104 ± 0.015	0.085 ± 0.013	16.2	McCarthy et al., 2013
Lake Erie	0.258 ± 0.128	0.036 ± 0.009	0.124 ± 0.052	19.9	McCarthy unpublished
Lake Okeechobee	0.577 ± 0.006	0.029 ± 0.01	0.160 ± 0.021	16.8	James et al. 2011
Taihu Lake	0.655 ± 0.285	0.271 ± 0.111	0.325 ± 0.144	11.5	McCarthy et al.2007
Taihu Lake	0.886 ± 0.09	0.399 ± 0.121	0.368 ± 0.071	37.4	This study
Lake Maracaibo	3.35 ± 0.795	2.73± 0.643	0.389 ± 0.175	22.0	Gardner et al. 1998

Table 4.
Details of best-fitting multiple regression models determined by stepwise regression. All rates, temperature, and ambient nutrient concentrations were log-transformed prior to analysis.

Process	Variable	Parameter			Model		
		Estimate	Std. estimate	P	Adj. R^2	F	P
Uptake Light	T	1.048	0.216	0.0001	0.643	10.3	9.14×10^{-6}
	DO	0.053	0.012	0.0002			
	pH	-0.320	0.054	0.0000			
	NH_4^+	0.669	0.272	0.0213			
Uptake Dark	T	0.488	0.121	0.0005	0.745	16.1	1.66×10^{-7}
	DO	0.034	0.007	0.0000			
	pH	-0.187	0.031	0.0000			
	NH_4^+	0.579	0.153	0.0008			
	NO_2^-	-1.619	0.660	0.0215			
	NO_3^-	-0.098	0.034	0.0086			
Regeneration	T	0.321	0.098	0.0031	0.695	12.8	1.42×10^{-6}
	DO	0.025	0.005	0.0003			
	pH	-0.092	0.024	0.0008			
	NH_4^+	0.386	0.126	0.0053			
	NO_3^-	-0.061	0.027	0.0340			
Nitrification	NO_2^-	3.262	1.226	0.0165	0.498	4.80	0.004

Figure 1


Liangxi River
Wuxi
Zhihu Gang
Wujin Gang
N
1
3
CH
TLLER
Yincun Gang
Wangyu River
7
Dapu Gang
10
Suzhou
Lake Taihu
Xu River
Jiapu River
Tiapu River
5km
CHINA
31° 24' N
Lake Taihu
120° 13' N
Changdou Gang
Daqian Gang
Legend
Surrounding River
Station Locations

Figure 2

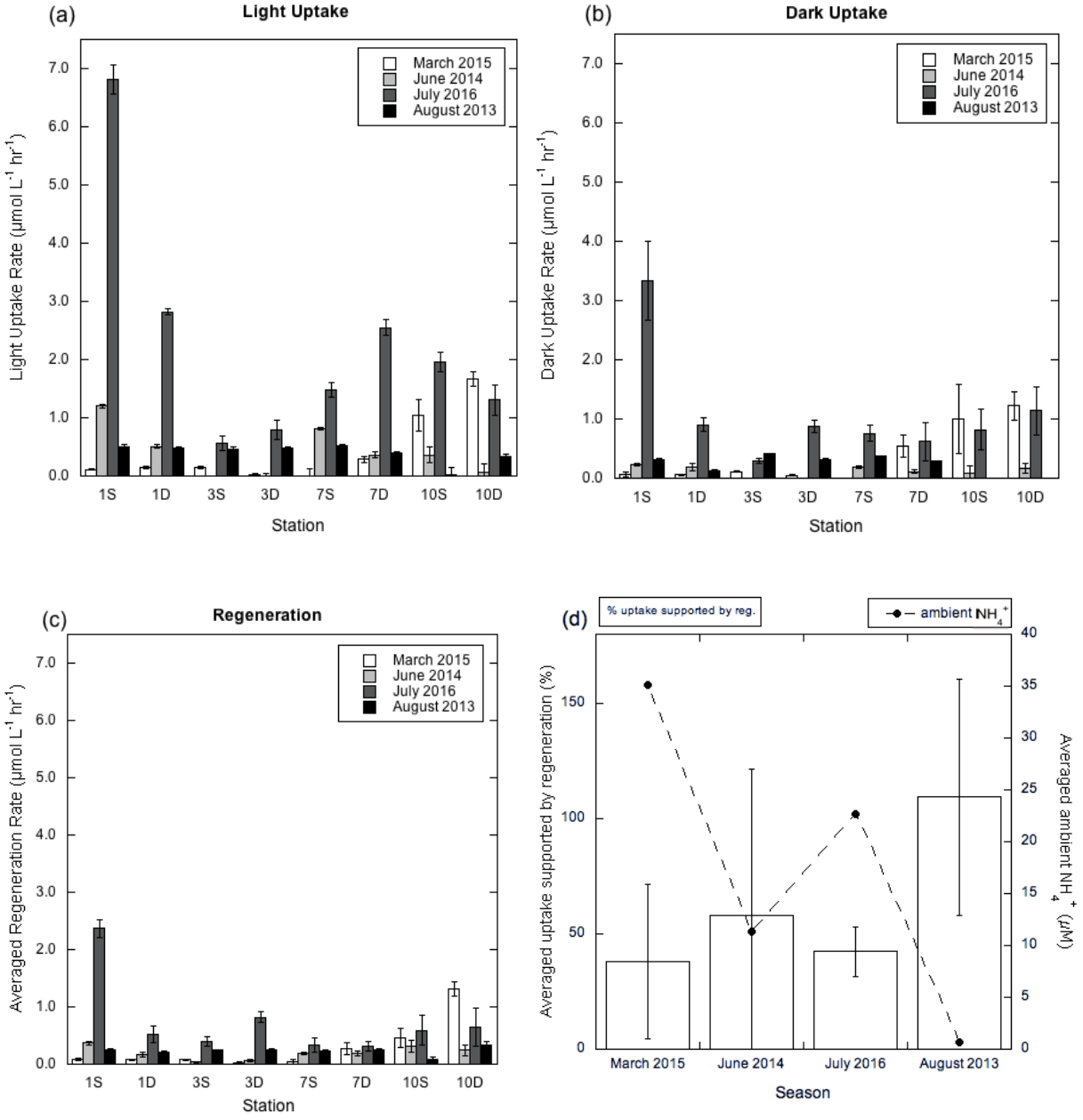
(a)
Light Uptake
March 2015
June 2014
July 2016
August 2013
Light Uptake Rate (µmol L-1 hr-1)
Station
1S
1D
3S
3D
7S
7D
10S
10D
(b)
Dark Uptake
Dark Uptake Rate (µmol L-1 hr-1)
(c)
Regeneration
Averaged Regeneration Rate (µmol L-1 hr-1)
(d)
% uptake supported by reg.
ambient NH4+
Averaged uptake supported by regeneration (%)
Averaged ambient NH4+ (µM)
Season
March 2015
June 2014
July 2016
August 2013

Figure 3

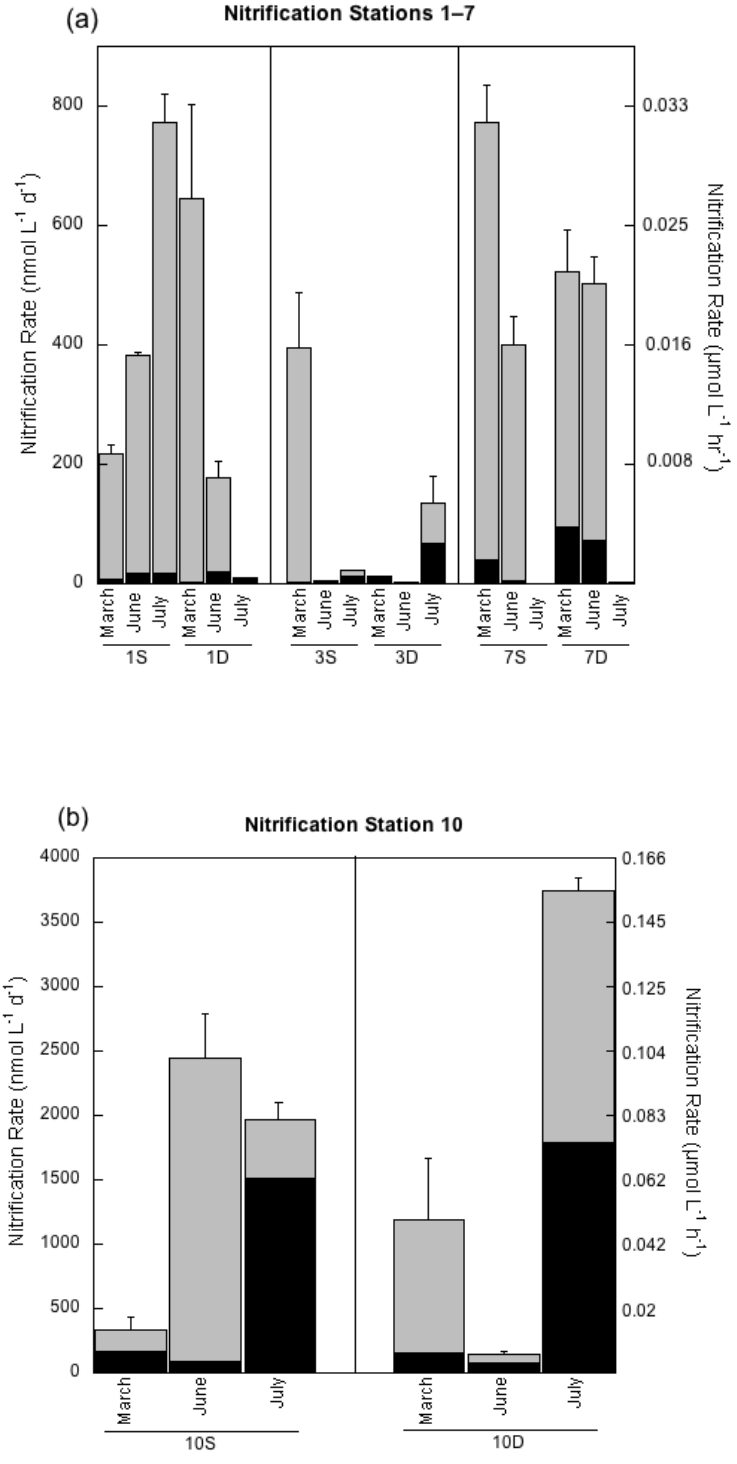
(a)
Nitrification Stations 1–7
Nitrification Rate (nmol L-1 d-1)
Nitrification Rate (µmol L-1 hr-1)
0
200
400
600
800
0.008
0.016
0.025
0.033
March
June
July
1S
1D
3S
3D
7S
7D
(b)
Nitrification Station 10
Nitrification Rate (nmol L-1 d-1)
Nitrification Rate (µmol L-1 h-1)
0
500
1000
1500
2000
2500
3000
3500
4000
0.02
0.042
0.062
0.083
0.104
0.125
0.145
0.166
10S
10D

Figure 4

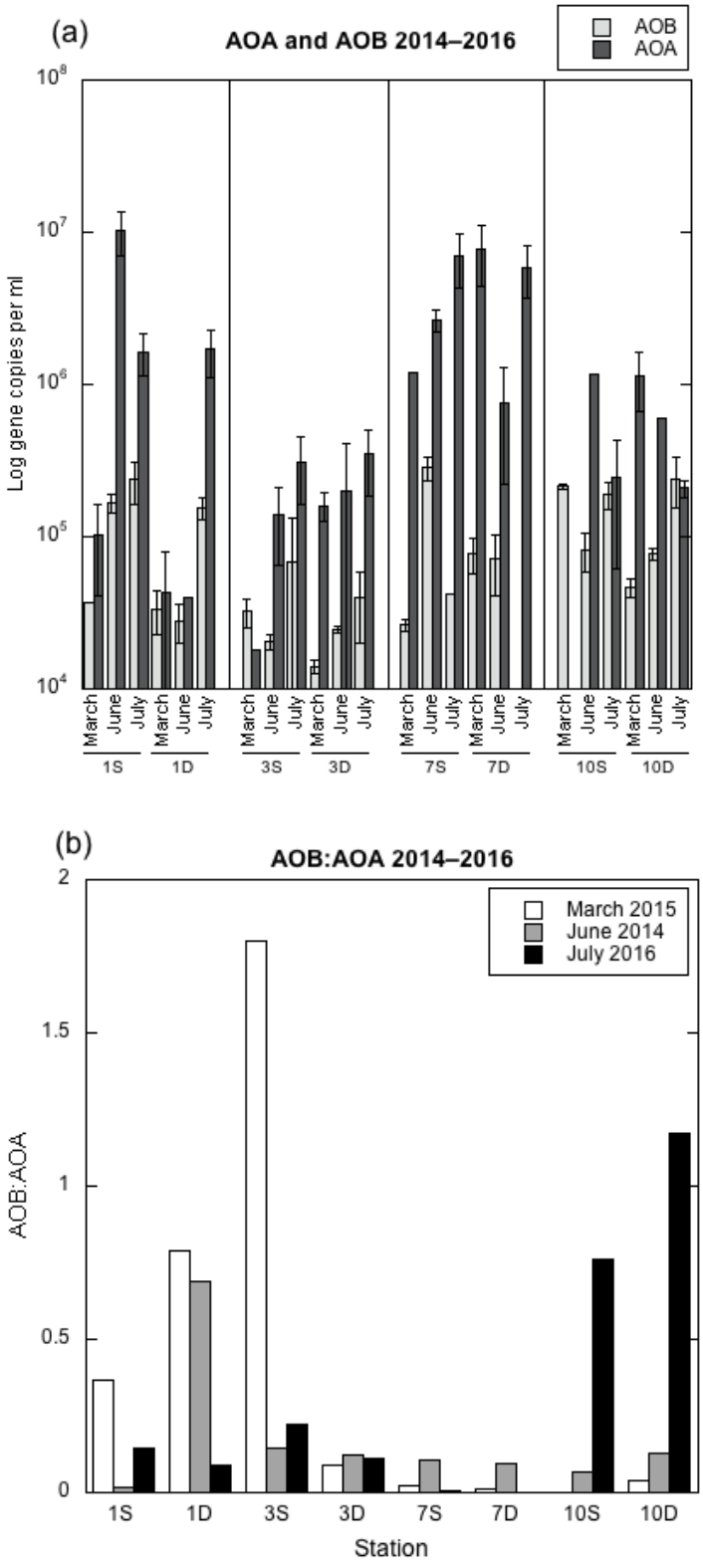
(a)
AOA and AOB 2014–2016
AOB
AOA
Log gene copies per ml
10^8
10^7
10^6
10^5
10^4
March
June
July
1S
1D
3S
3D
7S
7D
10S
10D
(b)
AOB:AOA 2014–2016
March 2015
June 2014
July 2016
AOB:AOA
2
1.5
1
0.5
0
1S
1D
3S
3D
7S
7D
10S
10D
Station